


Title	Circulating cell-free DNA-based epigenetic assay can detect early breast cancer
Author(s)	Uehiro, Natsue; Sato, Fumiaki; Pu, Fengling; Tanaka, Sunao; Kawashima, Masahiro; Kawaguchi, Kosuke; Sugimoto, Masahiro; Saji, Shigehira; Toi, Masakazu
Citation	Breast Cancer Research (2016), 18(1)
Issue Date	2016-12-19
URL	<a href="http://hdl.handle.net/2433/218380">http://hdl.handle.net/2433/218380</a>
Right	© The Author(s). 2016 Open Access This article is distributed under the terms of the Creative Commons Attribution 4.0 International License ( <a href="http://creativecommons.org/licenses/by/4.0/">http://creativecommons.org/licenses/by/4.0/</a> ), which permits unrestricted use, distribution, and reproduction in any medium, provided you give appropriate credit to the original author(s) and the source, provide a link to the Creative Commons license, and indicate if changes were made. The Creative Commons Public Domain Dedication waiver ( <a href="http://creativecommons.org/publicdomain/zero/1.0/">http://creativecommons.org/publicdomain/zero/1.0/</a> ) applies to the data made available in this article, unless otherwise stated.
Type	Journal Article
Textversion	publisher

RESEARCH ARTICLE

Open Access



# Circulating cell-free DNA-based epigenetic assay can detect early breast cancer

Natsue Uehiro<sup>1</sup>, Fumiaki Sato<sup>1\*</sup> , Fengling Pu<sup>2</sup>, Sunao Tanaka<sup>1</sup>, Masahiro Kawashima<sup>1</sup>, Kosuke Kawaguchi<sup>1</sup>, Masahiro Sugimoto<sup>3</sup>, Shigehira Saji<sup>2,4</sup> and Masakazu Toi<sup>1</sup>

## Abstract

**Background:** Circulating cell-free DNA (cfDNA) has recently been recognized as a resource for biomarkers of cancer progression, treatment response, and drug resistance. However, few have demonstrated the usefulness of cfDNA for early detection of cancer. Although aberrant DNA methylation in cfDNA has been reported for more than a decade, its diagnostic accuracy remains unsatisfactory for cancer screening. Thus, the aim of the present study was to develop a highly sensitive cfDNA-based system for detection of primary breast cancer (BC) using epigenetic biomarkers and digital PCR technology.

**Methods:** Array-based genome-wide DNA methylation analysis was performed using 56 microdissected breast tissue specimens, 34 cell lines, and 29 blood samples from healthy volunteers (HVs). Epigenetic markers for BC detection were selected, and a droplet digital methylation-specific PCR (ddMSP) panel with the selected markers was established. The detection model was constructed by support vector machine and evaluated using cfDNA samples.

**Results:** The methylation array analysis identified 12 novel epigenetic markers (*JAK3*, *RASGRF1*, *CPXM1*, *SHF*, *DNM3*, *CAV2*, *HOXA10*, *B3GNT5*, *ST3GAL6*, *DACH1*, *P2RX3*, and chr8:23572595) for detecting BC. We also selected four internal control markers (*CREM*, *GLYATL3*, *ELMOD3*, and *KLF9*) that were identified as infrequently altered genes using a public database. A ddMSP panel using these 16 markers was developed and detection models were constructed with a training dataset containing cfDNA samples from 80 HVs and 87 cancer patients. The best detection model adopted four methylation markers (*RASGRF1*, *CPXM1*, *HOXA10*, and *DACH1*) and two parameters (cfDNA concentration and the mean of 12 methylation markers), and was validated in an independent dataset of 53 HVs and 58 BC patients. The area under the receiver operating characteristic curve for cancer-normal discrimination was 0.916 and 0.876 in the training and validation dataset, respectively. The sensitivity and the specificity of the model was 0.862 (stages 0-I 0.846, IIA 0.862, IIB-III 0.818, metastatic BC 0.935) and 0.827, respectively.

**Conclusion:** Our epigenetic-marker-based system distinguished BC patients from HVs with high accuracy. As detection of early BC using this system was comparable with that of mammography screening, this system would be beneficial as an optional method of screening for BC.

**Keywords:** Circulating DNA, Breast cancer, Epigenetics, DNA methylation, Early detection

\* Correspondence: fsatoh@kuhp.kyoto-u.ac.jp

<sup>1</sup>Department of Breast Surgery, Graduate School of Medicine, Kyoto University, Kyoto, Japan

Full list of author information is available at the end of the article



## Background

Breast cancer (BC) is the most prevalent cancer and the leading cause of cancer deaths in women all over the world [1]. Currently, mammography is the standard method for early detection of BC in many countries. However, false-positive recall rates vary according to age, breast density, and postmenopausal hormonal therapy, among others [2, 3]. For women with dense breasts, the accuracy of mammography is decreased. As the breast density of Asian women is relatively high [4], there is an unmet need for the development of accurate BC screening methods. It is reported that ultrasonography helps to improve the sensitivity of detection in young Japanese women; however, there are some technical hurdles for standardization [5].

Blood-based methods for monitoring of BC have been in development for several decades. Conventional tumor markers, such as carcinoembryonic antigen (CEA), cancer antigen (CA)15-3 [6–8], and circulating tumor cell (CTC) count [9], are clinically available. However, their usefulness is mostly limited to patients with advanced and metastatic BC (MBC). Recently, circulating cell-free DNA (cfDNA) has received considerable attention as a resource of cancer biomarkers. Dawson et al. demonstrated that cfDNA-based markers (cancer-derived gene mutations) were more useful for monitoring metastatic BC than conventional tumor markers and CTC count [10]. As the cfDNA is thought to contain DNA derived from tumor cells in the whole body, tumor evolution can be also monitored by profiling the DNA mutation pattern.

Somatic gene mutations are highly specific events in cancer and precancerous lesions that can be useful in detecting cancer using remote samples. Technological approaches to quantifying tiny amounts of mutated DNA have been developed, such as digital PCR and barcode next-generation sequencing. However, in terms of cancer screening, next-generation sequencing is too expensive, and has a throughput capacity that is too low to process a large number of samples. In addition, detecting unknown mutated genes in cfDNA by a PCR-based method is difficult because mutation sites vary, even in highly mutated genes.

DNA methylation is an epigenetic system that regulates gene expression, and aberrant DNA methylation is associated with various pathologic events, including tumorigenesis and aggressive phenotypes of cancer. Since Silva et al. detected a methylated DNA fragment of the p16 promoter region in plasma samples from patients with BC [11], many reports have shown aberrantly-methylated DNA in plasma and serum [12–20]. However, the detection rates of these DNA methylation markers in the blood are low even in cases of advanced disease, and are therefore inadequate for early detection of BC [12, 13, 16–18]. In

the present study, we aimed to develop a highly sensitive cfDNA-based system for early detection of BC using epigenetic biomarkers and digital PCR technology.

## Methods

Detailed information on the materials and methods used in this study is provided in Additional file 1.

### Cell culture

The cell lines used in this study are listed in Additional file 2: Table S1. Cells were grown according to the distributors' recommended conditions.

### Collection of clinical samples

All blood and tissue samples were provided from a multi-institutional biobank project, the Breast Oncology Research Network (BORN)-Biobank, which was initiated and is maintained by the Department of Breast Surgery, Kyoto University. Blood samples from patients with BC were obtained after they received a traditional diagnosis of BC. In this study, BC stage 0-I was considered early BC.

### Laser capture microdissection (LMD) of BC tissue specimens

Individual 10- $\mu$ m-thick formalin-fixed paraffin-embedded (FFPE) specimens of surgically resected BC tissue were placed on Leica foil membrane slides, and immunohistochemically stained by pan-cytokeratin antibody cocktails (AE1/AE3, Dako, Glostrup, Denmark, M3515). Histo/Zyme (Diagnostic BioSystems, Pleasanton, CA, USA; DBS-K046-15) was used for antigen retrieval, and VECTOR Red Alkaline Phosphatase Substrate Kit (VECTOR Laboratories, Burlingame, CA, USA; SK-5100) was used for visualization. LMD of the stained FFPE slides was performed using LMD7000 systems (Leica microsystems, Wetzlar, Germany). Cancer cell clusters from the BC samples were selectively microdissected (Additional file 3: Figure S1). Normal samples obtained from adjacent normal mammary epithelia and intraductal papilloma epithelia were also microdissected. Adjacent normal epithelia from 10 patients were pooled as a single sample.

### Comprehensive DNA methylation profiling

Using an Illumina Infinium Human Methylation 450 BeadChip Assay (Illumina, San Diego, CA, USA), we conducted comprehensive DNA methylation profiling of 56 laser-microdissected FFPE samples (38 luminal, 4 luminal human epidermal growth factor receptor 2 (HER2), 1 HER2, and 11 triple-negative (TN) types of BC, one pooled normal epithelia sample, and one intraductal papilloma sample), 34 samples of DNA from 31 cultured cells (4 luminal, 3 luminal HER2, 2 HER2, and 18 TN types of BC, 1 unknown type of BC, and 3 non-BC cells), and 29 white blood cell DNA samples from

healthy volunteers (HVs), as listed in Additional file 2: Tables S1-S3. The peak bias in  $\beta$ -values of the two different probe types was corrected by an NIMBL toolbox [21] for MATLAB software.

At the selection of candidate markers, we attached importance to the difference of the methylation patterns based on the BC subtypes. To build a generalized multi-marker mathematical model for BC detection and avoid over-fitting, it is important to use several types of variables. Thus, we decided to select candidate markers from subtype-specific methylation loci, not only from loci commonly methylated in BC.

The mean  $\beta$ -values of the non-BC samples (meanNC), all BC samples (meanBC), and the luminal-type (meanLum) and TN-type (meanTN) of BC samples, were calculated. We selected the candidate markers from array probes with meanNC < 0.05. The additional selection conditions of the candidate markers were as follows; (a) top 20 loci of the widest gap between meanBC and meanNC; (b) top 20 loci of the lowest meanNC with meanBC > 0.6; (c) top 50 loci with the largest values of meanLum – meanTN; and (d) top 50 loci with the largest values of meanTN – meanLum. We referred to (a) and (b) as common BC markers, (c) as luminal-dominant markers, and (d) as TN-dominant markers. As the proportions of the cell lines and FFPE samples were different in the luminal and TN samples, direct calculation of the mean by sample type would be biased. To avoid such a bias, the mean  $\beta$ -values of each group were calculated as an average of the mean of the cell line samples and the mean of the FFPE samples. To evaluate the statistical significance of these markers, we calculated the  $p$  values using the Welch  $t$  test (Additional file 2: Table S4).

#### Screening of DNA methylation markers using real-time quantitative methylation-specific PCR (MSP)

We used the Taqman-based MSP method in this screening step. To save screening costs and time, we utilized the Universal Probe Library (UPL, Roche Diagnostics GmbH, Mannheim, Germany) to design Taqman-MSP primers and probes. As the sequence variety of UPLs is limited, we designed primers and probes as close as possible to the candidate loci selected by the methylation array analysis (Additional file 2: Table S4). The MSP reaction mix consisted of 10  $\mu$ l of FastStart Universal Probe Master (ROX) (Roche Diagnostics GmbH), 1  $\mu$ l of primer mix for MSP (finally 0.5  $\mu$ M), 0.4  $\mu$ l of UPL probe, 2  $\mu$ l of template bisulfite-treated DNA, and H<sub>2</sub>O up to 20  $\mu$ l in total. The PCR reaction was performed using the StepOnePlus Real-Time PCR System (Applied Biosystems, Foster City, CA, USA) as follows; one cycle at 95 °C for 10 minutes, fifty cycles at 95 °C for 15 sec and 60 °C for 1 minute. A standard curve was generated using serially diluted, fully methylated DNA synthesized

by SssI methyltransferase (New England Biolabs, Ipswich, MA, USA), and methylation values were normalized by MSP values of the *ACTB* gene as previously described [22].

Primers were selected on the basis of the following: (1) the efficiency of MSP was >70% and <110%; (2) methylation was detected in one or none of the samples of blood DNA from HVs; (3) methylation was detected in more than one sample of the DNA from the cultured cell lines; (4) methylation was not detected in the DNA derived from FFPE samples of adjacent normal epithelia; and (5) expression of the related genes was regulated by DNA methylation.

#### Validation of candidate DNA methylation markers with the public database

To evaluate the universality of candidate markers, we analyzed the methylation data of peripheral blood mononuclear cells (PBMC, GSE58888) [23], and BC in The Cancer Genome Atlas (TCGA) Project [24] generated by the TCGA Research Network (<http://cancergenome.nih.gov/>). Then we showed the methylation pattern of samples with candidate markers in a heat map format. The distributions of the  $\beta$ -values for the selected methylation markers were compared among PBMC samples, all cancer samples, luminal BC samples, and basal-like BC samples using the Welch  $t$  test.

#### Pharmacological unmasking of epigenetically silenced genes

To determine whether the expression of the screened marker genes was epigenetically regulated, MCF7, T47D, MDA-MB-231, and Hs578T were treated with the demethylating agent 5'-Aza-2-deoxycytidine (5'-Aza-dC) (Sigma-Aldrich, St. Louis, MO, USA) at 1  $\mu$ M for 48 hours, and both 5'-Aza-dC and histone deacetylase inhibitor trichostatin A (Sigma-Aldrich) at 300 nM for 24 hours. DNA and RNA samples were then extracted. The methylation status of each selected marker was measured by quantitative MSP, as described. The RNA expression level of each gene was assessed by one-step reverse transcription PCR (RT-PCR) using a QuantiTect Probe RT-PCR Master Mix (QIAGEN, Venlo, Netherlands) according to the manufacturer's protocol.

#### Establishing the MSP assay using droplet digital PCR

To quantify tiny amounts of methylated DNA in cfDNA, we employed droplet digital PCR. To adjust selected primer/probe sets to duplex droplet digital PCR format, custom dual-labeled locked nucleic acid probes with FAM or Alexa Fluor® 532 dye and Black hole-1 quencher were synthesized for certain markers (Gene Design Inc., Ibaraki, Osaka, Japan). The final sequences of MSP primers and probes for selected markers are listed in Additional file 2: Table S5.

In epigenetic research, a primer/probe set developed by Eads et al., which targets the upstream region of *ACTB* [22], was traditionally used as an internal control reaction of MSP and also used in marker screening steps. However, in this study, the amplification efficiency of this primer/probe set was not sufficient. In addition, because the amounts of loaded cfDNA samples in droplet digital methylation-specific PCR (ddMSP) reactions are unknown and considerably varied, precise quantification is very important in an assay detection system. Therefore, we developed a panel of four novel internal control markers. We selected four internal control genes of which the copy number alteration ratios were less than 5%, according to the cBioPortal database (<http://cbioportal.org>) [25, 26]. The primer/probe sets for internal control markers were designed to target genomic regions containing no CpG, in order to amplify the region regardless of methylation status (Additional file 2: Table S6).

#### Detecting methylated DNA markers in cfDNA by ddMSP

The extraction of cfDNA from plasma was conducted using QIAmp Circulating Nucleic Acid Kit (QIAGEN) with a modification of the manufacturer's protocol to improve the cfDNA yield. Briefly, 900  $\mu$ l of thawed plasma was mixed with 100  $\mu$ l of PBS, 800  $\mu$ l of Buffer ACL (lysis buffer), and 100  $\mu$ l of proteinase K solution, and then was incubated at 48 °C for 18 hours with shaking. The sample was then mixed with an additional 100  $\mu$ l of proteinase K solution by pulse-vortexing for 30 seconds, and was incubated for a further 6 hours. Finally, approximately 20  $\mu$ l of cfDNA solution was eluted.

Following the manufacturer's protocol, duplex ddMSP reactions were performed in a T100 thermal cycler (Bio-Rad, Hercules, CA, USA), and droplet signals were quantified by a QX100™ Droplet Reader (Bio-Rad). In total, 278 cfDNA samples from 145 patients with BC and 133 HVs were analyzed using this ddMSP assay, and all raw droplet signal data were exported from the built-in software, and manually analyzed using MATLAB software as follows.

#### Data analysis of ddMSP data and development of the detection model

First, a sample dataset of 278 cases was randomly divided into a training set ( $n = 167$ ) and a validation set ( $n = 111$ ), each set being in accordance with the proportion of cancer patients and HVs, and with BC stage. Clinicopathological characteristics of the patients for cfDNA are shown in Table 1 and Additional file 2: Table S7. A detection algorithm was developed using the training dataset only. For each marker, optimized lower and upper cutoff thresholds for droplet amplitude were determined to maximize the area under the curve (AUC) of the receiver

operator characteristic (ROC) curve as a single marker. The concentration of the methylated marker DNA fragments (copies/ml) was then calculated for each sample. The cutoff concentration for each marker was determined to divide the samples into marker-negative and marker-positive groups. All marker concentration values were converted into log10 values. Thus, the whole training dataset consisted of a total of 15 variables, including the concentration values of 12 DNA methylation markers and their mean value, a mean of four internal control markers, and the number of methylation-positive markers.

We developed a BC detecting model using a support vector machine (SVM) to distinguish patients with cancer from HVs. To determine the best variable set for the model, we tested all of the variable combinations ( $n = 2^{15} - 1$ ). For each combination, the detection accuracy was estimated by leave-one-out cross-validation (LOOCV). The model that achieved the best AUC and coefficients of each variable that were  $>0$ , was then selected as the detection model.

To validate the robustness of the selected model, an independent dataset was used. The validation dataset was prepared using thresholds of droplet signals and cutoffs for marker concentration determined by the training dataset. The best SVM model selected above was applied to the validation data set. The accuracy of the detection model for the validation set was assessed using the AUC. Furthermore, we also performed ROC analysis and calculated the AUC to evaluate the performance of the model within each stage of BC as a subgroup analysis.

#### Statistical analysis

Methylation assay analysis, processing of ddMSP data, and algorithm construction were performed using MATLAB software. Statistical analyses, such as correlation analysis, tendency analysis, and *t* statistics, among others, were performed using R software.

## Results

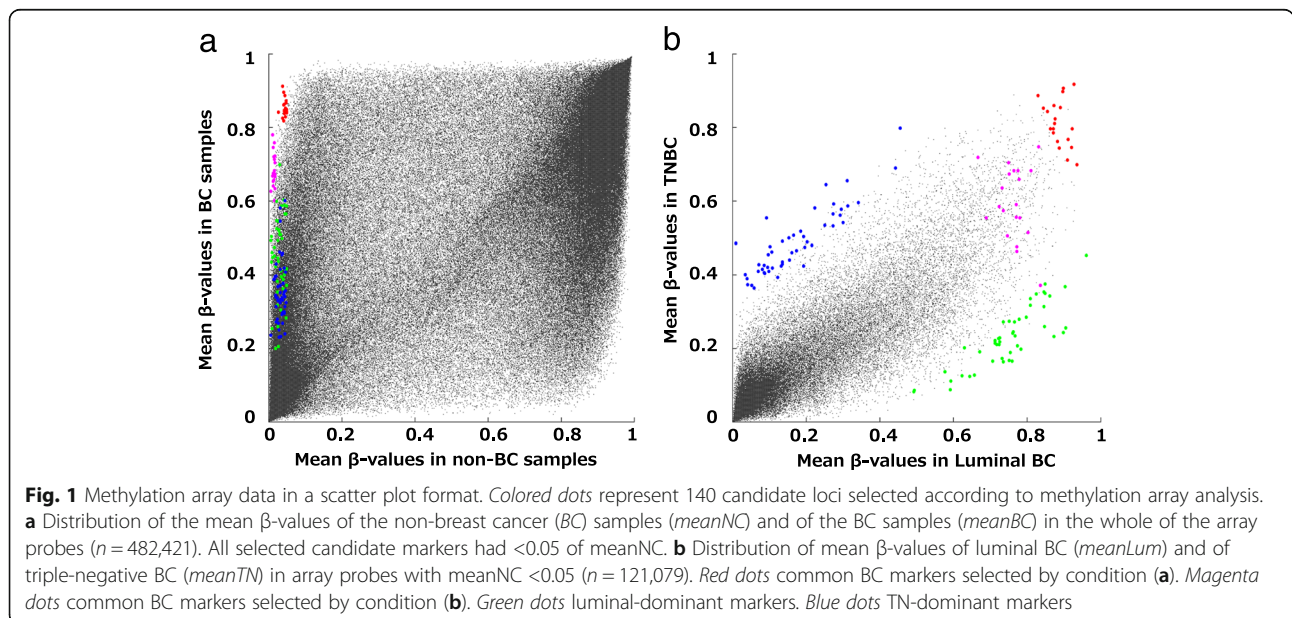
#### Comprehensive DNA methylation array analysis

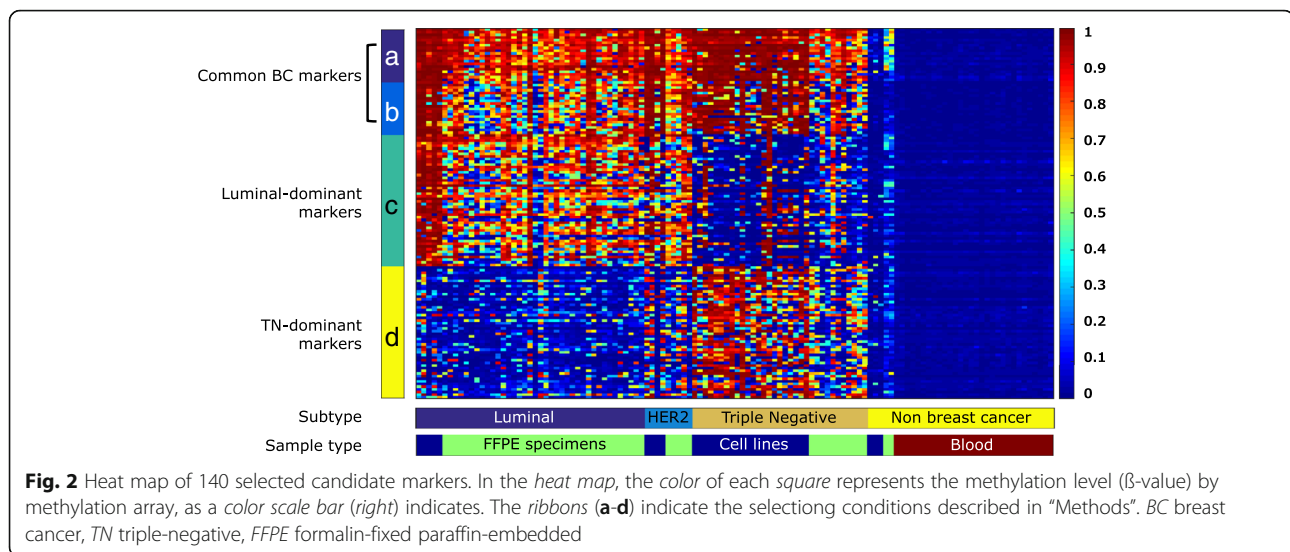
According to DNA methylation array data, a total of 140 candidate markers, including 40 common BC markers, 50 luminal-dominant markers, and 50 TN-dominant markers, were selected. Figure 1 shows the distribution of meanNC and meanBC among the whole of the array probes ( $n = 482,421$ ), and the distribution of meanLum and meanTN in the array probes with meanNC  $<0.05$  ( $n = 121,079$ ). The colored dots represent the selected 140 candidate markers. The methylation values of these markers are shown in a heat map format in Fig. 2. All the selected candidates had a low methylation status in the non-BC samples ( $\beta$ -value  $<0.05$ ), shown in blue. Some of the luminal-dominant marker candidates were highly methylated, even in the TN samples, probably because the

**Table 1** Characteristics of healthy volunteers and patients with breast cancer

		Whole set (n = 278)	Training set (n = 167)	Validation set (n = 111)
Number of samples	HVs	133	80	53
	Patients with BC	145	87	58
Mean age (range)	HVs	45.3 (22–70)	45.8 (26–70)	44.5 (22–66)
	Patients with BC	59.5 (36–81)	59.8 (36–81)	59.1 (36–81)
Subtype	Luminal	98	58	40
	Triple-negative	25	14	11
	HER2	10	6	4
	Luminal HER2	8	6	2
	not assessed (DCIS)	4	3	1
Stage	0	4	3	1
	I	47	27	20
	IIA	31	19	12
	IIB	22	11	11
	III	9	8	1
Early BC (Stage0-I)	IV	32	19	13
	Luminal	36	22	14
	Triple-negative	8	3	5
	HER2	2	2	0
	Luminal HER2	1	0	1
	not assessed (DCIS)	4	3	1

HVs healthy volunteers, BC breast cancer, HER2 human epidermal growth factor receptor 2, DCIS ductal carcinoma in situ, Subtype immunohistochemically categorized subtype





luminal androgen-receptor-positive subtype samples may be included in these TN samples.

#### Validation of candidate DNA methylation markers using the public database

As the number of samples of FFPE tissue specimens was relatively small, we validated the methylation status of the candidate markers using relatively large public datasets. There were 143 samples of PBMC in GSE 58888 [23] and 610 samples of BC in TCGA [24] datasets using the Illumina Infinium Human Methylation 450 Bead-Chip Assay platform. In 610 samples of TCGA data, we analyzed 213 samples which were linked with subtype information of PAM50. In the BC samples, the numbers of samples in the luminal A, luminal B, HER2-enriched, normal-like, and basal-like subtypes were 140, 46, 14, 5, and 40, respectively. A heat map generated using these datasets demonstrated that luminal A/B and PBMC samples had a similar methylation pattern to our luminal samples and blood samples (Additional file 3: Figure S2A). The basal-like subtype in PAM50 and the clinical TN subtype are not identical but partially overlapped; they also had a similar methylation pattern in our analysis. Although the TCGA samples were not laser-microdissected, the methylation pattern was similar, which indicated that methylation marker status would not be affected by the contaminated stromal cells.

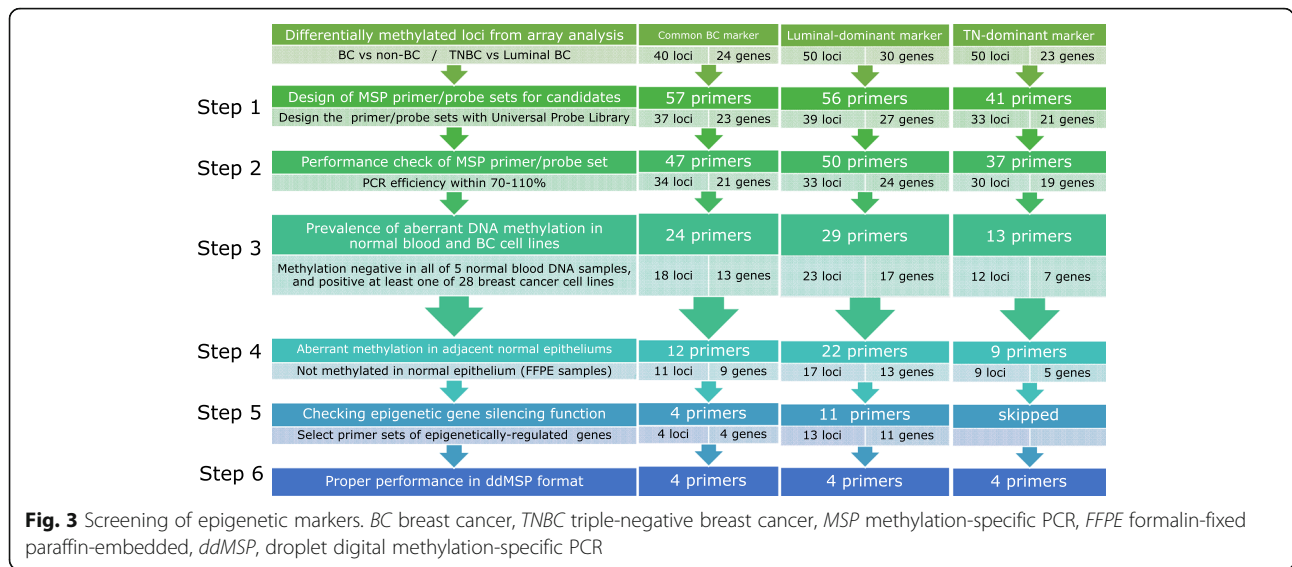
#### Screening of selected candidate markers

The steps for screening the selected candidate markers are illustrated in Fig. 3. Briefly, the screening steps included (1) a primer/probe quality check, (2) quantitative MSP screening using BC cell lines and normal blood samples, (3) quantitative MSP screening using laser-microdissected FFPE samples of normal epithelia, (4)

checking the gene silencing function of candidate markers, and (5) checking the signal amplitude pattern in ddMSP reactions. We selected *JAK3*, Ras-specific guanine nucleotide-releasing factor 1 (*RASGRF1*), carboxypeptidase X (*CPXMI*), and Src homology 2 domain-containing adapter protein F (*SHF*) as the common BC markers, Dynamin 3 (*DNM3*), Caveolin 2 (*CAV2*), Homeobox protein Hox-A10 (*HOXA10*), and *B3GNT5* as the luminal-dominant markers, and *ST3GAL6*, Dachshund homolog 1 (*DACH1*), P2X purinoceptor 3 (*P2RX3*), and chr8:23572595 as the TN-dominant markers (Table 2, Additional file 2: Tables S4 and S5). DNA methylation status and a differentially methylated region in the genomic area surrounding the selected markers are illustrated in Additional file 3: Figure S3. For the common BC markers and the luminal-dominant markers, we selected the markers possessing an epigenetic gene silencing function (Additional file 3: Figures S4 and S5). Selected subtype-specific methylation markers are statistically significantly differentially methylated in the luminal and basal subtypes in the TCGA dataset [24] (Additional file 3: Figure S2-B).

#### Performance of the internal control marker panel

In this study, we adopted an internal control marker panel to assess the concentration of cfDNA in the plasma sample. For precise assessment of cfDNA concentration, the markers should not be affected by copy number alteration (CNA) of the cancer genome. Therefore, we chose four markers (cAMP-responsive element modulator (*CREM*), Glycine N-acyltransferase-like protein 3 (*GLYATL3*), ELMO/CED-12 domain containing 3 (*ELMOD3*), and Kruppel-like factor 9 (*KLF9*)), for which the CNA rates were less than 5% in BC, according to the cBioPortal database. A geometric mean of four markers



represented the cfDNA concentration of the samples. We compared the performance of this internal control panel and conventional *ACTB* primer/probe in the ddMSP assay system, using white blood cell DNA samples derived from 16 HVs and 16 patients with BC

(Additional file 3: Figure S6). There was good correlation between cfDNA concentration measured by this panel and by *ACTB*. However, the amounts of cfDNA detected by the panel were significantly higher than by the *ACTB* primer/probe set.

**Table 2** Epigenetic markers employed in the ddMSP assay

Gene	Name	Product length	Chr	CpG
Common BC markers				
<i>JAK3</i>	Tyrosine-protein kinase JAK3	129	19	s-shore
<i>RASGRF1</i>	Ras-specific guanine nucleotide-releasing factor 1	104	15	island
<i>CPXM1</i>	Carboxypeptidase X1	94	20	island
<i>SHF</i>	Src homology 2 domain-containing adapter protein F	117	15	island
Luminal-dominant markers				
<i>DNM3</i>	Dynamin 3	105	19	n-shore
<i>CAV2</i>	Caveolin 2	141	7	island
<i>HOXA10</i>	Homeobox protein Hox-A10	135	7	island
<i>B3GNT5</i>	UDP-GlcNAc:betaGal beta-1,3-N acetylglucosaminyltransferase 5	97	3	island
TN-dominant markers				
<i>ST3GAL6</i>	ST3 beta-galactoside alpha-2,3-sialyltransferase 6	82	3	s-shore
<i>DACH1</i>	Dachshund homolog 1	110	13	n-shore
<i>P2RX3</i>	P2X purinoceptor 3	118	11	island
Chr8:23572595	Intergenic locus corresponding to probe cg23495581, located at chr 8: 23,572,595 in GRCh37	83	8	s-shore
Internal control markers for MSP				
<i>CREM</i>	cAMP-responsive element modulator	75	10	
<i>GLYATL3</i>	Glycine N-acyltransferase-like protein 3	107	6	
<i>ELMOD3</i>	ELMO/CED-12 domain containing 3	90	2	
<i>KLF9</i>	Kruppel-like factor 9	89	9	

ddMSP droplet digital methylation-specific PCR, Chr chromosome, island CpG island, shore CpG shore (region within 2000 bps from CpG island), n-shore/s-shore northern/southern CpG shore (CpG shore attached to upstream/downstream side of CpG island, respectively), GRC Genome Reference Consortium



### Development of a BC detection model using the ddMSP system

First, the detection performance of each variable was assessed by univariate analysis (Additional file 3: Figure S7A and B). The AUC for methylation markers in the ROC analysis ranged from 0.56 to 0.71. The AUC of each internal control surpassed 0.80, and the AUC for the mean of the internal controls was 0.89. The AUCs for the mean value of the 12 methylation markers and the number of positive methylated markers were 0.77 and 0.82, respectively.

Optimization of variable combinations is important to obtain a detection model with high accuracy. In this study, we tested all of the possible combinations using 15 variables ( $n = 2^{15} - 1$ ) by the LOOCV method. The SVM model using *RASGRF1*, *CPXM1*, *HOXA10*, and *DACH1*, the mean of 12 markers, and the mean of the internal controls had the highest AUC of 0.92, thus, we selected this variable combination from the detection models. The sensitivity and specificity of this model was 0.91 and 0.83, respectively (Additional file 2: Table S8). The equation of the selected SVM model is expressed below:

$$\begin{aligned} \text{Detection index} = & 0.62449 \times [\text{RASGRF1}] + 0.78110 \\ & \times [\text{CPXM1}] + 0.12115 \times [\text{HOXA10}] \\ & + 0.36760 \times [\text{DACH1}] + 0.65288 \\ & \times [\text{Mean12}] + 2.44704 \times [\text{IC}] - 6.98073 \end{aligned}$$

where [RASGRF1], [CPXM1], [HOXA10], [DACH1], [Mean12], and [IC] represented the log<sub>10</sub> concentration of the methylated DNA fragments of *RASGRF1*, *CPXM1*, *HOXA10*, *DACH1* gene loci, mean concentration of 12 methylation markers, and the mean concentration of four internal control markers, respectively. According to the ROC curve analysis, samples with a detection index of more than  $-0.07923$  were defined as positive for BC. All the ddMSP data are shown in Additional file 2: Table S7 and are also presented in a heat map format (Fig. 4a and Additional file 3: Figure S7C). The pattern of IC was similar to that of the detection index, which indicated that the IC largely contributed to the detection index. However, their patterns were not the same. Thus, other epigenetic markers might contribute to increasing specificity of the model.

As a validation study, the developed SVM model was applied to the validation dataset. The AUC, sensitivity, and specificity of the validation set were 0.88, 0.84, and 0.79, respectively. Using all the data, the sensitivity and specificity of this model was 0.88 and 0.81, respectively. In addition, the positive/negative predictive values and accuracy of the model was 0.84, 0.85, and 0.85, respectively (Additional file 2: Table S8). The ROC curves of the selected model for the training and validation sets are shown in Fig. 4b.

### Age bias in the detection index in patients with BC

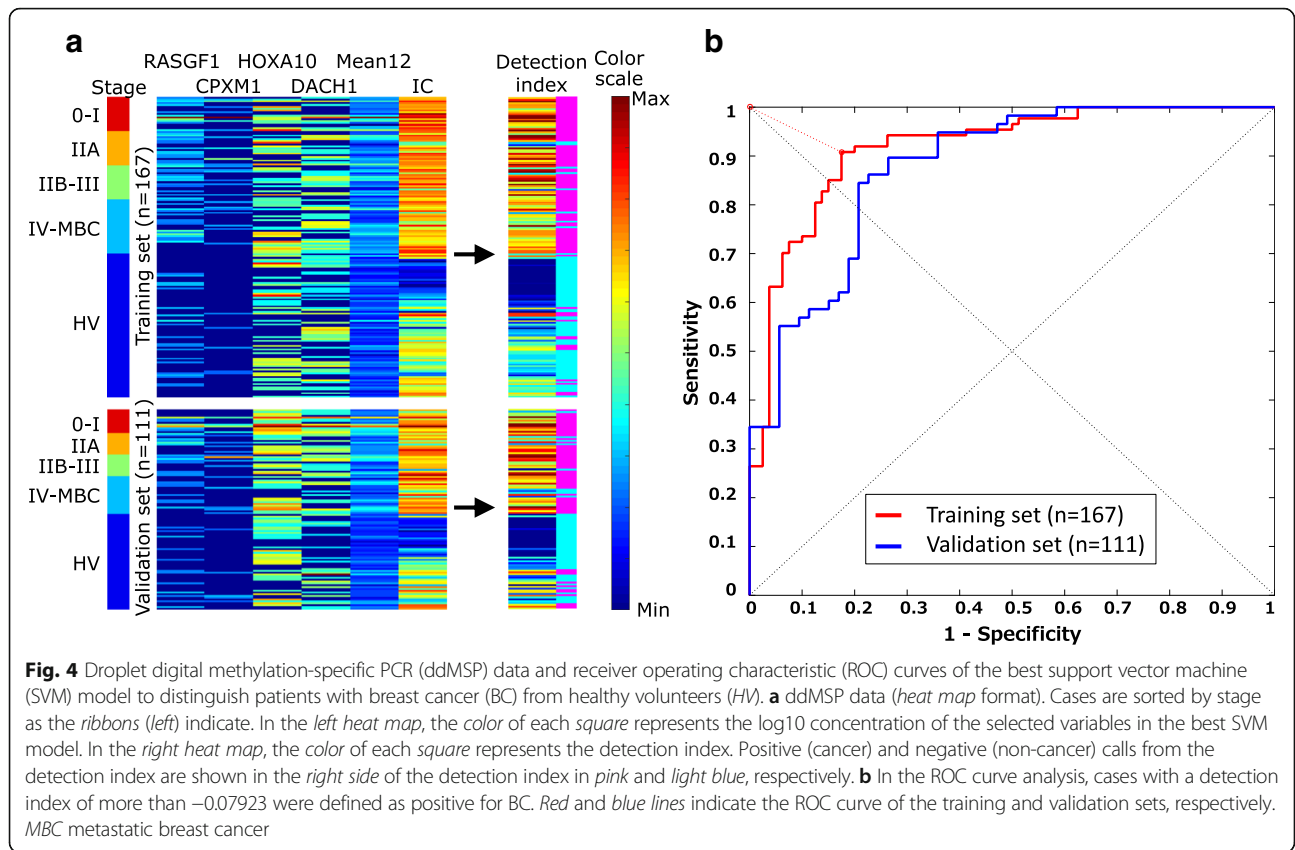
The cells of elderly individuals tend to be hypermethylated, compared to the cells of younger individuals. In addition, the HVs who participated in this study were significantly younger than the patients with BC. To determine whether the detection accuracy of this model was biased by age, we tested correlation between the detection index and age in the BC samples. As shown in a scatter plot (Additional file 3: Figure S8), there was almost no relationship between age and the detection index (Pearson's correlation,  $r = 0.075$ ,  $p = 0.39$ ). There was weak but significant correlation between age and 3 out of the 12 markers, and as a single marker (Additional file 2: Table S9). Among the six variables employed in the fixed model, only *RASGRF1* was biased by age. This may be the reason why the detection index was not biased by age as a whole.

### Correlation between stage, subtype, and the detection index

There was a statistically significant trend toward a higher detection index in advanced-stage BC samples (Jonckheere-Terpstra (JT) test,  $p = 0.0087$ ) (Fig. 5). However, this did not mean that the samples in the early stages tended to be diagnosed as false negatives. All four patients with ductal carcinoma in situ (DCIS) and 85% of patients with stage-I BC were correctly categorized into the cancer group. For more detail, in 41 of the 47 patients with stage-I cancer, the size of the primary tumor was recorded; the sensitivity for patients with T1a ( $n = 2$ ), T1b ( $n = 12$ ), and T1c ( $n = 27$ ) BC was 1, 0.83, and 0.85, respectively. Furthermore, the AUC of ROC analysis of early BC was 0.911 in the training set and 0.854 in the validation set, which was comparable with the AUC for advanced BC, ranging from 0.896 to 0.960 in the training set, and from 0.881 to 0.901 in the validation set (Additional file 3: Figure S9).

The research aim of this study was to develop a tool for the early detection of BC. Thus, the detection accuracy in these early-stage samples would have significant impact for future clinical application. As our detection index correlated with the stage of BC, the index might indicate the prognosis of patients with BC. However, all of the cfDNA samples were collected after December 2011. Thus, the follow-up period was too short to derive any statistical conclusions about survival in BC.

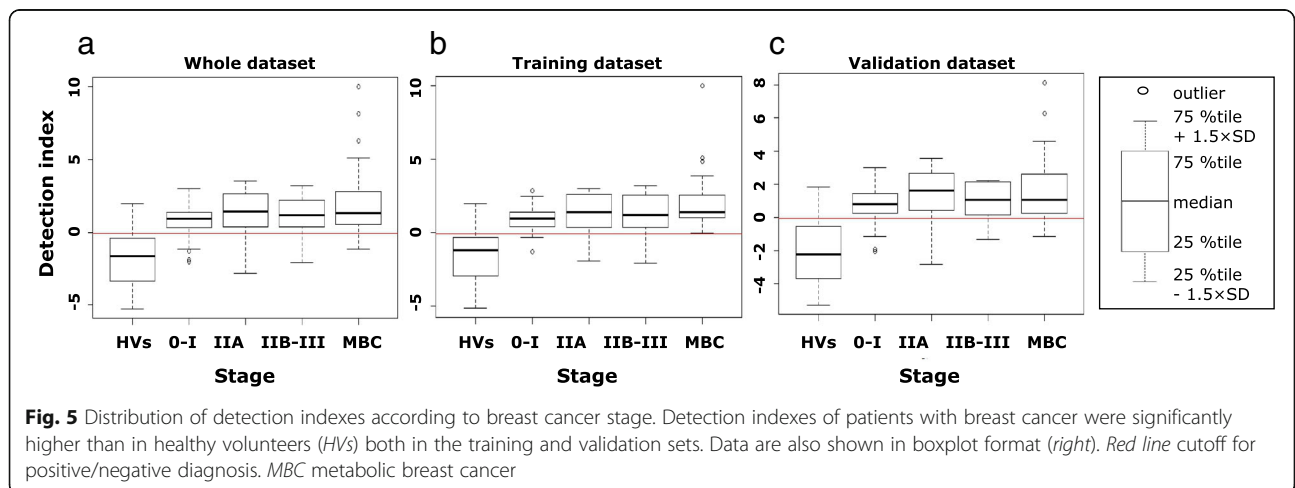
The detection index did not differ among the four BC subtypes (Kruskal-Wallis test,  $p = 0.074$ ) (Fig. 6a). In the TN BC cases, there was also a significant trend toward a higher detection index in samples from patients in the advanced stage of BC (JT test,  $p = 0.021$ ) (Fig. 6c), whereas there was no such significant trend in the patients with luminal BC (JT test,  $p = 0.05$ ) (Fig. 6b). There was also no trend in the patients with HER2

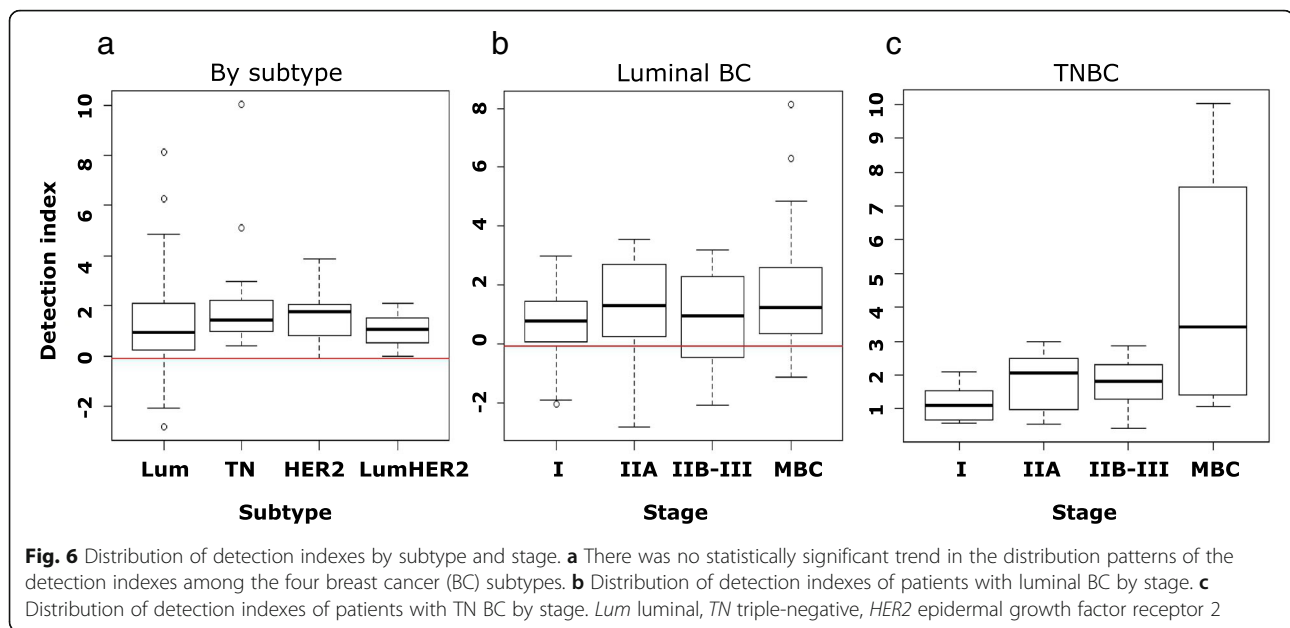


and luminal HER2 BC (JT test,  $p = 0.20$  and  $p = 0.81$ , respectively), which is likely due to the small sample size (Additional file 3: Figure S10).

All the TN, HER2, and luminal HER2 BC samples, even those at stage I, were stratified into the cancer group. In contrast, 17 out of the 98 luminal BC samples (17.3%) were falsely stratified into the non-cancer group,

which contained some advanced/metastatic cases (Fig. 5). Limited to the early stage, 7 patients (19.4%) were diagnosed as non-cancer. In the 17 false-negative patients, 15 had  $>50\%$  estrogen-receptor-positive cells, and 13 also had  $>20\%$  progesterone-receptor-positive cells in primary tumors. Furthermore, the Ki-67 index of 10 false-negative patients was under 14%. Taken together, the





fixed model had relatively lower detection accuracy for the luminal A-like subtype [27] of BC samples than that for the other subtype samples.

## Discussion

In this study, we developed a cfDNA-based system for early diagnosis of BC using an epigenetic marker panel. Most previous studies of DNA methylation markers in cfDNA for BC utilized the MSP method by real-time PCR, and obtained a wide range of diagnostic accuracy, as shown in Additional file 2: Table S10 [12–15, 17–20]. Generally, methylation markers were detected frequently in patients with metastatic BC, unlike in patients with early BC, in whom methylation markers were less frequent.

In comparison with other studies, our study had unique and advantageous key points. First, we selected epigenetic markers from genome-wide screening by array analysis, whereas most previous studies chose markers in a knowledge-based way. Screening novel markers from genome-wide analysis required considerable effort to identify the final markers; however, this method may have a better chance of obtaining accurate marker sets than the knowledge-based method. Furthermore, we validated the results of our methylation array analysis, using large sample cohorts of PBMC samples [23] and TCGA BC samples [24]. This validation analysis confirmed that selected candidate markers were differentially methylated among subtypes in independent datasets.

Second, we employed the cfDNA concentration data in the detection algorithm to improve detection performance. The mean IC, which represented the cfDNA

concentration, largely contributed to the high accuracy of the algorithm. Third, our model was highly accurate even in the detection of patients with early BC. The sensitivity of detection in patients with BC stage 0-I was 90.0% in the training set and 81.0% in the validation set. The ROC of AUC for this stage was 0.911 in the training set, and 0.854 in the validation set. In the previous studies conducted in the USA, Europe, and Asia, the sensitivity and specificity of mammography ranged from 74.6 to 92.5% and from 83.1 to 99.5%, respectively [5, 28–30]. In addition, the sensitivity and specificity of mammography in women aged 40–49 years was lower than in women aged 50–70 years [2]. Taking into consideration that 42% of patients ( $n = 117$ ) in this study was below 50 years of age, the detection of early BC by our model was comparable with that of mammography. Thus, these results indicated that our system could be an optional method in BC mass screening in the future. Finally, we validated the accuracy of the fixed model using a large cohort ( $n = 111$ ). We proved that our system could have generalized potential to distinguish patients with BC from HVs.

Similar to other reports, each methylation marker in this study had low-range to mid-range sensitivity. The low sensitivity is reasonable because we intentionally selected luminal-dominant and TN-dominant markers that were unmethylated in the other subtypes. In general, the keys to building a good multi-marker mathematical model for prediction or diagnosis include avoiding overfitting to obtain a generalized model, and covering as large a variety of data patterns as possible. According to the results of the TCGA Project [24] and the Carolina Breast Cancer Study [31], there are some subtypes

within the DNA methylation pattern. If we chose markers only by sensitivity as a single marker, epigenetic data from these markers would be redundant and would miss some important features. Thus, we intentionally selected subtype-specific markers, not only common BC markers. Adding different types of information, such as mean methylation values and a cfDNA concentration measured by internal control markers, helped to improve the accuracy of the model. Moreover, the numbers of variables are important. The model should include enough data to accurately show the potential variety without overfitting the model. Sixteen markers, the number used in our model, would be a reasonable size, and feasible in terms of clinical application by the PCR-based assay system, similar to Oncotype Dx [32].

Markers targeting four genes were employed in the fixed model. Three of the four genes were recognized as tumor suppressor genes according to previous functional studies. *RASGRF1* activates Ras by stimulating the dissociation of GDP from RAS protein. *RASGRF1/2* regulates Cdc42-mediated tumor cell transformation and cell motility, working as a tumor suppressor gene [33]. Hypermethylation in the promoter region of *RASGRF1* has been observed in gastric cancer cells and precancerous tissues of the gastric mucosae [34]. Our report is the first to show that the *RASGRF1* promoter region is hypermethylated in both the luminal and TN BC subtypes.

*CPXMI*, also known as *CPXI*, encodes a metalloproteinase protein. Although one study reported that *CPXMI* may regulate osteoclastogenesis in mice [35], its function in human cancer cells remains unknown. Our analysis indicates that its expression is epigenetically regulated, and it may act as a tumor suppressor gene in BC cells. However, further functional studies are required to confirm its function.

*HOXA10* encodes one of the DNA-binding transcription factors that regulate gene expression, morphogenesis and differentiation, functioning as a tumor suppressor gene. *HOXA10* is methylated in differentiated CD24-positive normal mammary cells and luminal BC cells [36], and the methylation level increases during the progression of BC from DCIS via a primary invasive ductal carcinoma, to a metastatic tumor [36, 37]. These data are consistent with our results, that *HOXA10* is a luminal-dominant marker.

*DACHI* encodes a chromatin-associated protein that regulates gene expression and cell fate determination during development, and also functions as a tumor suppressor gene. *DACHI* is epigenetically silenced in colorectal and hepatocellular carcinoma [38, 39]. In BC, *DACHI* represses aggressive characteristics such as stem cell function, epithelial-mesenchymal transition, migration activity, and so on [40–45]. Moreover, *DACHI* expression is higher in the luminal subtype than in the

basal subtype [42, 43, 46]. These facts support our observation that *DACHI* is selected as a TN-dominant methylation marker.

This panel also contained four novel internal control markers for MSP to measure cfDNA concentration precisely. The primer/probe sets were designed to target DNA sequences with no CpGs. In this study, the mean value of these internal controls had a good AUC, which largely contributed to the high detection accuracy of the developed SVM model. This finding was consistent with previous articles showing that the cfDNA concentration in patients with BC was significantly higher than that of HVs [47–50]. However, the methods in these previous results have not been implemented in BC screening. As the quantity of DNA was measured by spectrophotometry or PCR in these studies, the data may not have been accurate enough to detect early BC. In the present study, we employed a digital PCR system to enable absolute quantification of the amount of cfDNA and aberrantly methylated DNA fragments. The mean of the internal controls had a high AUC as a single marker, contributing to the development of a more accurate algorithm by adding information to cfDNA methylation data. According to the cBioPortal data, the genes of the internal control markers were mutated, amplified, and lost in less than 5% of other malignancies [25, 26]. Thus, this internal control panel could be beneficial for the detection of other types of cancer as well.

On the other hand, this ddMSP-based detection system has some limitations. First, there were 23 (15.5%) false positives among the HVs. Although methylation markers were selected with an emphasis on specificity, some methylation markers have low specificity. One explanation is the non-specific elevation of cfDNA concentration. In fact, the cfDNA concentration in the false-positive HVs was significantly higher than the true-negative HVs (Additional file 3: Figure S11). According to the coefficients of the model equation, the contribution of cfDNA concentration to the detection index is large. Thus, elevated cfDNA concentration caused by non-cancerous events such as inflammation or a benign cell-proliferative lesion may result in a false-positive diagnosis. Another possible reason is the existence of a pre-diagnostic malignant lesion, and not only BC. Our clinical data contained the BC screening results of the HVs by imaging and physical examination, which could not deny the existence of pre-diagnostic BC or other malignancies. Longitudinal analysis using serially obtained samples is required to check whether false-positive individuals have such lesions. However, the false-positive rate in this study was within a comparable level to current BC screening methods based on clinical breast examination and imaging, such as mammography and ultrasonography, with specificity ranging from 6.9 to 19.6% [2, 3, 5].

Second, there were 17 (17.3%) false-negative patients with luminal BC, which included some with advanced/metastatic BC, and 7 (19.4%) were limited to early BC. The false-negative patients had low mean values of 12 methylated markers ( $t$  test,  $p < 0.0001$ ) and low cfDNA concentration ( $t$  test,  $p < 0.0001$ ) (Additional file 3: Figure S11). Ten false-negative patients were categorized as having the luminal A-like subtype of BC. Due to the fact that in patients with cancer, cfDNA may consist of circulating tumor DNA derived from the necrotic or apoptotic tumor cells and cell-free DNA from cells in the tumor microenvironment, luminal BC with low proliferation and low activity in its tumor microenvironment might produce relatively low cfDNA, and may cause false-negative diagnosis.

Pepe, et al., statisticians in the Early Detection Research Network (EDRN), defined five phases of screening biomarker development, and described the aims, study design, and evaluation methods for each phase. According to these definitions, this study was in phase 1 (preclinical exploratory studies) and phase 2 (clinical assay development for clinical disease) [51]. The usefulness of this system in the BC screening setting should be demonstrated in the later phases. According to our results, this detection system for BC seems to be worthwhile for advancement into the next phase.

The original objective of this system was early detection of BC for screening purposes. However, this system can be applied to clinical uses other than for detection of BC. Previous DNA methylation studies using cfDNA demonstrated that methylation status of several genes was different at baseline in responders and non-responders to therapy, and the methylated DNA marker decreased in responders during therapy [16]. In the present study, as cfDNA samples in the more advanced stages had a higher detection index, the index represented tumor burden. Thus, this ddMSP system could also be a useful tool to monitor the therapeutic response of metastatic BC. Furthermore, this panel could distinguish early TN BC, and could have potential as an alternative to screening by magnetic resonance imaging in patients and carriers of the *BRCA*-mutation. These issues will be investigated in a further study.

## Conclusion

We established an epigenetic marker panel for cfDNA and a detection algorithm to distinguish patients with BC from HVs with high accuracy. As the detection of early BC using this system was comparable with mammography screening, this cfDNA-based detection system would be beneficial as an option for BC screening. A further study is necessary to demonstrate its clinical usefulness as an optional method for BC screening.

## Additional files

**Additional file 1:** This file provides detailed materials and methods for this study. (DOCX 66 kb)

**Additional file 2: Table S1.** Characteristics of cell lines used in this study. **Table S2.** Characteristics of FFPE samples used in methylation array analysis. **Table S3.** Characteristics of healthy volunteers in methylation array analysis. **Table S4.** Primer/probe set designed for methylation markers. **Table S5.** Sequence of primer/probe sets for methylation markers. **Table S6.** Sequence of primer/probe sets of internal control markers. **Table S7.** Clinical data of cfDNA samples and results of ddMSP analysis. **Table S8.** Sensitivity and specificity of the best SVM model. **Table S9.** Correlation between age and each marker/parameter. **Table S10.** Summary of recent epigenetic studies regarding cfDNA for BC. **Table S11.** Upper and lower cutoff threshold of positive droplets. **Table S12.** Cutoffs of marker concentration to categorize into marker-positive/negative groups. **Table S13.**  $P$  values of statistical tests in the validation analysis using public datasets. (XLSX 172 kb)

**Additional file 3: Figure S1.** Laser microdissection of pan-cytokeratin (AE1/AE3)-immunostained FFPE specimens. **Figure S2.** A-B Validation analysis using large public datasets. **Figure S3.** A-L DNA methylation status in genomic region surrounding candidate marker loci, and differentially methylated region. **Figure S4.** Unmasking of epigenetically silenced genes by demethylating agent and histone deacetylase inhibitor (common BC markers). **Figure S5.** Unmasking of epigenetically silenced genes by demethylating agent and histone deacetylase inhibitor (luminal-dominant markers). **Figure S6.** Relationship between *ACTB* and the new panel of internal control markers. **Figure S7.** A-C ROC curves and ddMSP data of 12 methylation markers and three parameters. **Figure S8.** Detection index and age. **Figure S9.** ROC curves in each stage of BC. **Figure S10.** Distribution of detection indexes of HER-positive patients by stage. **Figure S11.** cfDNA concentration in HVs and patients with BC. **Figure S12.** A-E Determining upper and lower thresholds for positive droplets. (PPTX 12394 kb)

## Abbreviations

5'-Aza-dC: 5'-Aza-2-deoxycytidine; AUC: area under the curve; BC: breast cancer; BORN: Breast Oncology Research Network; cfDNA: circulating cell-free DNA; CNA: copy number alteration; *CPXM1*: carboxypeptidase X (M14 family) member1; *CREM*: cAMP-responsive element modulator; CTC: circulating tumor cell; *DACH1*: Dachshund family transcription factor 1; DCIS: ductal carcinoma in situ; ddMSP: droplet digital methylation-specific PCR; *ELMOD3*: ELMO/CEB-12 domain containing 3; FFPE: formalin-fixed paraffin-embedded; *GLYATL3*: glycine N-acyltransferase-like protein 3; HER2: human epidermal growth factor receptor 2; *HOXA10*: homeobox A10; HV: healthy volunteer; JT test: Jonckheere-Terpstra test; *KLF9*: Kruppel-like factor 9; LMD: laser microdissection; LOOCV: leave-one-out cross-validation; MBC: metastatic breast cancer; meanBC: mean  $\beta$ -values in all breast cancer samples; meanLum: mean  $\beta$ -values in luminal-type BC samples; meanNC: mean  $\beta$ -values of the non-breast cancer samples; meanTN: mean  $\beta$ -values in the triple-negative breast cancer samples; MSP: methylation-specific PCR; PBMC: peripheral blood mononuclear cells; PBS: phosphate-buffered saline; ROC: receiver operating characteristic; RT-PCR: reverse transcription PCR; SVM: support vector machine; TCGA: The Cancer Genome Atlas; TN: triple negative; UPL: Universal Probe Library

## Acknowledgements

We thank all of the BORN BioBank participants, including Kazuyo Fujimura, Hiroyasu Nishizawa, and Yasuyuki Shimahara at Yamato Koriyama Hospital, Ryuji Okamura at Yamato Takada Municipal Hospital, Takashi Okino at Kohga Public Hospital, Shigeru Tsuyuki at Osaka Red Cross Hospital, Mitsuru Tanaka at Hirakata Kohsai Hospital, Hirofumi Suwa at Hyogo Prefectural Amagasaki General Medical Center, Akira Yamauchi at Kitano Hospital, and their colleagues, for collecting clinical samples and data. We thank Junji Itou, Haruko Takuwa, Marina Kiso, and Wen Zhao Li for discussing the interpretation of the data.

### Funding

This research was funded by the Project for Development of Innovative Research on Cancer Therapeutics (P-DIRECT)/Ministry of Education, Culture, Sports, Science and Technology of Japan and was partly supported by the Princess Takamatsu Cancer Research Fund.

### Availability of data and material

A supplemental file of information on materials and methods is downloadable from the journal's website. The raw and peak-based corrected beta-value data of the Illumina methylation array is deposited in the Gene Expression Omnibus (GEO) [52] database of NCBI [GEO:GSE87177].

### Authors' contributions

NU, FS, SS, and MT conceived the study, participated in its design, and prepared the manuscript. NU carried out the cell culture, tissue microdissection and molecular epigenetic studies, interpreted the data, and drafted the manuscript. FP carried out the cell culture and immunostaining of FFPE samples. ST carried out the cell culture. FS and MS carried out the construction of the algorithm and the statistical analyses. MK and KK collected clinical samples as responsible persons of the biobank. All authors have read and approved the final manuscript.

### Competing interest

The authors declare that they have no competing interests.

### Consent for publication

All authors agreed the final version of the manuscript for publication.

### Ethics approval and consent to participate

This study was approved by the Ethical Committee of Kyoto University Hospital (Protocol number: G534). All blood and tissue samples were provided from a multi-institutional biobank project, the BORN-Biobank, which was initiated and is maintained by the Department of Breast Surgery, Kyoto University. The protocol of this biobank project was approved by the ethical committees of all the participating institutions. All samples were originally obtained from patients with BC and HVs who had visited participating institutions, and were collected and stored in the Department of Breast Surgery, Kyoto University. Written informed consent forms for comprehensive research use were obtained from all patients and HVs.

### Author details

<sup>1</sup>Department of Breast Surgery, Graduate School of Medicine, Kyoto University, Kyoto, Japan. <sup>2</sup>Department of Target Therapy Oncology, Graduate School of Medicine, Kyoto University, Kyoto, Japan. <sup>3</sup>Institute for Advanced Biosciences, Keio University, Tsuruoka, Yamagata, Japan. <sup>4</sup>Department of Medical Oncology, Fukushima Medical University, Fukushima, Japan.

Received: 5 April 2016 Accepted: 1 December 2016

Published online: 19 December 2016

### References

- Torre LA, Bray F, Siegel RL, Ferlay J, Lortet-Tieulent J, Jemal A. Global cancer statistics, 2012. *CA Cancer J Clin*. 2015;65(2):87–108.
- Suzuki A, Kuriyama S, Kawai M, Amari M, Takeda M, Ishida T, et al. Age-specific interval breast cancers in Japan: estimation of the proper sensitivity of screening using a population-based cancer registry. *Cancer Sci*. 2008;99(11):2264–7.
- Kerlikowske K, Zhu W, Hubbard RA, Geller B, Dittus K, Braithwaite D, et al. Outcomes of screening mammography by frequency, breast density, and postmenopausal hormone therapy. *JAMA Intern Med*. 2013;173(9):807–16.
- del Carmen MG, Halpern EF, Kopans DB, Moy B, Moore RH, Goss PE, et al. Mammographic breast density and race. *Am J Roentgenol*. 2007;188(4):1147–50.
- Ohuchi N, Suzuki A, Sobue T, Kawai M, Yamamoto S, Zheng Y-F, et al. Sensitivity and specificity of mammography and adjunctive ultrasonography to screen for breast cancer in the Japan Strategic Anti-cancer Randomized Trial (J-START): a randomised controlled trial. *Lancet*. 2015;387(10016):341–8.
- Duffy MJ, Evoy D, McDermott EW. CA 15-3: uses and limitation as a biomarker for breast cancer. *Clin Chim Acta*. 2010;411(23–24):1869–74.
- Fu Y, Li H. Assessing clinical significance of serum CA15-3 and carcinoembryonic antigen (CEA) levels in breast cancer patients: a meta-analysis. *Med Sci Monit*. 2016;22:3154–62.
- Graham LJ, Shupe MP, Schneble EJ, Flynt FL, Clemenshaw MN, Kirkpatrick AD, et al. Current approaches and challenges in monitoring treatment responses in breast cancer. *J Cancer*. 2014;5(1):58–68.
- Bidard FC, Peeters DJ, Fehm T, Nole F, Gisbert-Criado R, Mavroudis D, et al. Clinical validity of circulating tumour cells in patients with metastatic breast cancer: a pooled analysis of individual patient data. *Lancet Oncol*. 2014;15(4):406–14.
- Dawson SJ, Tsui DW, Murtaza M, Biggs H, Rueda OM, Chin SF, et al. Analysis of circulating tumor DNA to monitor metastatic breast cancer. *N Engl J Med*. 2013;368(13):1199–209.
- Silva JM, Dominguez G, Villanueva MJ, Gonzalez R, Garcia JM, Corbacho C, et al. Aberrant DNA methylation of the p16INK4a gene in plasma DNA of breast cancer patients. *Br J Cancer*. 1999;80(8):1262–4.
- Hoque MO, Feng Q, Toure P, Dem A, Critchlow CW, Hawes SE, et al. Detection of aberrant methylation of four genes in plasma DNA for the detection of breast cancer. *J Clin Oncol*. 2006;24(26):4262–9.
- Mirza S, Sharma G, Prasad CP, Parshad R, Srivastava A, Gupta SD, et al. Promoter hypermethylation of TMS1, BRCA1, ERalpha and PRB in serum and tumor DNA of invasive ductal breast carcinoma patients. *Life Sci*. 2007;81(4):280–7.
- Brooks JD, Cairns P, Shore RE, Klein CB, Wvirgin I, Afanasyeva Y, et al. DNA methylation in pre-diagnostic serum samples of breast cancer cases: results of a nested case-control study. *Cancer Epidemiol*. 2010;34(6):717–23.
- Radpour R, Barekati Z, Kohler C, Lv Q, Burki N, Diesch C, et al. Hypermethylation of tumor suppressor genes involved in critical regulatory pathways for developing a blood-based test in breast cancer. *PLoS One*. 2011;6(1):e16080.
- Sharma G, Mirza S, Parshad R, Gupta SD, Ralhan R. DNA methylation of circulating DNA: a marker for monitoring efficacy of neoadjuvant chemotherapy in breast cancer patients. *Tumour Biol*. 2012;33(6):1837–43.
- Chimonidou M, Strati A, Malamos N, Georgoulas V, Lianidou ES. SOX17 promoter methylation in circulating tumor cells and matched cell-free DNA isolated from plasma of patients with breast cancer. *Clin Chem*. 2013;59(1):270–9.
- Kloten V, Becker B, Winner K, Schrauder MG, Fasching PA, Anzeneder T, et al. Promoter hypermethylation of the tumor-suppressor genes ITH5, DKK3, and RASSF1A as novel biomarkers for blood-based breast cancer screening. *Breast Cancer Res*. 2013;15(1):R4.
- Martinez-Galan J, Torres-Torres B, Nunez MI, Lopez-Penalver J, Del Moral R, Ruiz De Almodovar JM, et al. ESR1 gene promoter region methylation in free circulating DNA and its correlation with estrogen receptor protein expression in tumor tissue in breast cancer patients. *BMC Cancer*. 2014;14:59.
- Fackler MJ, Lopez Bujanda Z, Umbricht C, Teo WW, Cho S, Zhang Z, et al. Novel methylated biomarkers and a robust assay to detect circulating tumor DNA in metastatic breast cancer. *Cancer Res*. 2014;74(8):2160–70.
- Wessely F, Emes RD. Identification of DNA methylation biomarkers from Infinium arrays. *Front Genet*. 2012;3:161.
- Eads CA, Danenberg KD, Kawakami K, Saltz LB, Blake C, Shibata D, et al. MethyLight: a high-throughput assay to measure DNA methylation. *Nucleic Acids Res*. 2000;28(8):E32.
- Marttila S, Kananen L, Hayrynen S, Jylhava J, Nevalainen T, Hervonen A, et al. Ageing-associated changes in the human DNA methylome: genomic locations and effects on gene expression. *BMC Genomics*. 2015;16:179.
- Network CGA. Comprehensive molecular portraits of human breast tumours. *Nature*. 2012;490(7418):61–70.
- Cerami E, Gao J, Dogrusoz U, Gross BE, Sumer SO, Aksoy BA, et al. The cBio cancer genomics portal: an open platform for exploring multidimensional cancer genomics data. *Cancer Discov*. 2012;2(5):401–4.
- Gao J, Aksoy BA, Dogrusoz U, Dresdner G, Gross B, Sumer SO, et al. Integrative analysis of complex cancer genomics and clinical profiles using the cBioPortal. *Sci Signal*. 2013;6(269):11.
- Goldhirsch A, Winer EP, Coates AS, Gelber RD, Piccart-Gebhart M, Thurlimann B, et al. Personalizing the treatment of women with early breast cancer: highlights of the St Gallen International Expert Consensus on the Primary Therapy of Early Breast Cancer 2013. *Ann Oncol*. 2013;24(9):2206–23.
- Hofvind S, Geller BM, Skelly J, Vacek PM. Sensitivity and specificity of mammographic screening as practised in Vermont and Norway. *Br J Radiol*. 2012;85(1020):e1226–32.
- Kemp Jacobsen K, O'Meara ES, Key D, Buist SMD, Kerlikowske K, Vejborg I, et al. Comparing sensitivity and specificity of screening mammography in the United States and Denmark. *Int J Cancer*. 2015;137(9):2198–207.
- Lee K, Kim H, Lee JH, Jeong H, Shin SA, Han T, et al. Retrospective observation on contribution and limitations of screening for breast cancer

- with mammography in Korea: detection rate of breast cancer and incidence rate of interval cancer of the breast. *BMC Womens Health*. 2016;16(1):72.
31. Conway K, Edmiston SN, May R, Kuan PF, Chu H, Bryant C, et al. DNA methylation profiling in the Carolina Breast Cancer Study defines cancer subclasses differing in clinicopathologic characteristics and survival. *Breast Cancer Res*. 2014;16(5):450.
  32. Paik S, Shak S, Tang G, Kim C, Baker J, Cronin M, et al. A multigene assay to predict recurrence of tamoxifen-treated, node-negative breast cancer. *N Engl J Med*. 2004;351(27):2817–26.
  33. Calvo F, Sanz-Moreno V, Agudo-Ibanez L, Wallberg F, Sahai E, Marshall CJ, et al. RasGRF suppresses Cdc42-mediated tumour cell movement, cytoskeletal dynamics and transformation. *Nat Cell Biol*. 2011;13(7):819–26.
  34. Takamaru H, Yamamoto E, Suzuki H, Nojima M, Maruyama R, Yamano HO, et al. Aberrant methylation of RASGRF1 is associated with an epigenetic field defect and increased risk of gastric cancer. *Cancer Prev Res (Phila)*. 2012;5(10):1203–12.
  35. Chang EJ, Kwak HB, Kim H, Park JC, Lee ZH, Kim HH. Elucidation of CPX-1 involvement in RANKL-induced osteoclastogenesis by a proteomics approach. *FEBS Lett*. 2004;564(1-2):166–70.
  36. Bloushtain-Qimron N, Yao J, Snyder EL, Shipitsin M, Campbell LL, Mani SA, et al. Cell type-specific DNA methylation patterns in the human breast. *Proc Natl Acad Sci U S A*. 2008;105(37):14076–81.
  37. Park SY, Kwon HJ, Lee HE, Ryu HS, Kim SW, Kim JH, et al. Promoter CpG island hypermethylation during breast cancer progression. *Virchows Arch*. 2011;458(1):73–84.
  38. Zhu H, Wu K, Yan W, Hu L, Yuan J, Dong Y, et al. Epigenetic silencing of DACH1 induces loss of transforming growth factor-beta1 antiproliferative response in human hepatocellular carcinoma. *Hepatology*. 2013;58(6):2012–22.
  39. Yan W, Wu K, Herman JG, Brock MW, Fuks F, Yang L, et al. Epigenetic regulation of DACH1, a novel Wnt signaling component in colorectal cancer. *Epigenetics*. 2013;8(12):1373–83.
  40. Popov VM, Zhou J, Shirley LA, Quong J, Yeow WS, Wright JA, et al. The cell fate determination factor DACH1 is expressed in estrogen receptor-alpha-positive breast cancer and represses estrogen receptor-alpha signaling. *Cancer Res*. 2009;69(14):5752–60.
  41. Wu K, Katiyar S, Li A, Liu M, Ju X, Popov VM, et al. Dachshund inhibits oncogene-induced breast cancer cellular migration and invasion through suppression of interleukin-8. *Proc Natl Acad Sci U S A*. 2008;105(19):6924–9.
  42. Wu K, Jiao X, Li Z, Katiyar S, Casimiro MC, Yang W, et al. Cell fate determination factor Dachshund reprograms breast cancer stem cell function. *J Biol Chem*. 2011;286(3):2132–42.
  43. Wu K, Chen K, Wang C, Jiao X, Wang L, Zhou J, et al. Cell fate factor DACH1 represses YB-1-mediated oncogenic transcription and translation. *Cancer Res*. 2014;74(3):829–39.
  44. Zhao F, Wang M, Li S, Bai X, Bi H, Liu Y, et al. DACH1 inhibits SNAI1-mediated epithelial-mesenchymal transition and represses breast carcinoma metastasis. *Oncogenesis*. 2015;4:e143.
  45. Wu K, Li A, Rao M, Liu M, Dailey V, Yang Y, et al. DACH1 is a cell fate determination factor that inhibits cyclin D1 and breast tumor growth. *Mol Cell Biol*. 2006;26(19):7116–29.
  46. Chen K, Wu K, Gormley M, Ertel A, Wang J, Zhang W, et al. Acetylation of the cell-fate factor dachshund determines p53 binding and signaling modules in breast cancer. *Oncotarget*. 2013;4(6):923–35.
  47. Zhong XY, Ladewig A, Schmid S, Wight E, Hahn S, Holzgreve W. Elevated level of cell-free plasma DNA is associated with breast cancer. *Arch Gynecol Obstet*. 2007;276(4):327–31.
  48. Silva JM, Silva J, Sanchez A, Garcia JM, Dominguez G, Provencio M, et al. Tumor DNA in plasma at diagnosis of breast cancer patients is a valuable predictor of disease-free survival. *Clin Cancer Res*. 2002;8(12):3761–6.
  49. Perkins G, Yap TA, Pope L, Cassidy AM, Dukes JP, Riisnaes R, et al. Multi-purpose utility of circulating plasma DNA testing in patients with advanced cancers. *PLoS One*. 2012;7(11):e47020.
  50. Jahr S, Hentze H, Englisch S, Hardt D, Fackelmayr FO, Hesch RD, et al. DNA fragments in the blood plasma of cancer patients: quantitations and evidence for their origin from apoptotic and necrotic cells. *Cancer Res*. 2001;61(4):1659–65.
  51. Pepe MS, Etzioni R, Feng Z, Potter JD, Thompson ML, Thornquist M, et al. Phases of biomarker development for early detection of cancer. *J Natl Cancer Inst*. 2001;93(14):1054–61.
  52. Edgar R, Domrachev M, Lash AE. Gene Expression Omnibus: NCB gene expression and hybridization array data repository. *Nucleic Acids Res*. 2002;30(1):207–10.

Submit your next manuscript to BioMed Central and we will help you at every step:

- We accept pre-submission inquiries
- Our selector tool helps you to find the most relevant journal
- We provide round the clock customer support
- Convenient online submission
- Thorough peer review
- Inclusion in PubMed and all major indexing services
- Maximum visibility for your research

Submit your manuscript at  
[www.biomedcentral.com/submit](http://www.biomedcentral.com/submit)

